MOLECULAR AND CELLULAR BIOLOGY, July 2007, p. 4774–4783 Vol. 27, No. 13
0270-7306/07/$08.00+0 doi:10.1128/MCB.00283-07

Ubiquitination-Induced Conformational Change within the Deiodinase Dimer Is a Switch Regulating Enzyme Activity▽

G. D. Vivek Sagar,[1]† Balázs Gereben,[2]† Isabelle Callebaut,[3] Jean-Paul Mornon,[3] Anikó Zeöld,[2] Wagner S. da Silva,[1] Cristina Luongo,[1] Monica Dentice,[1] Susana M. Tente,[1] Beatriz C. G. Freitas,[1] John W. Harney,[1] Ann Marie Zavacki,[1] and Antonio C. Bianco[1]*

Thyroid Section, Division of Endocrinology, Diabetes and Hypertension, Brigham and Women's Hospital, Harvard Medical School, Boston, Massachusetts 02115[1]; Laboratory of Endocrine Neurobiology, Institute of Experimental Medicine, Hungarian Academy of Sciences, Budapest H-1083, Hungary[2]; and Département de Biologie structurale, IMPMC, CNRS UMR7590, Universities Paris 6 and Paris 7, Paris 75252 Cedex 05, France[3]

Received 15 February 2007/Returned for modification 11 April 2007/Accepted 13 April 2007

Ubiquitination is a critical posttranslational regulator of protein stability and/or subcellular localization. Here we show that ubiquitination can also regulate proteins by transiently inactivating enzymatic function through conformational change in a dimeric enzyme, which can be reversed upon deubiquitination. Our model system is the thyroid hormone-activating type 2 deiodinase (D2), an endoplasmic reticulum-resident type 1 integral membrane enzyme. D2 exists as a homodimer maintained by interacting surfaces at its transmembrane and globular cytosolic domains. The D2 dimer associates with the Hedgehog-inducible ubiquitin ligase WSB-1, the ubiquitin conjugase UBC-7, and VDU-1, a D2-specific deubiquitinase. Upon binding of T4, its natural substrate, D2 is ubiquitinated, which inactivates the enzyme by interfering with D2's globular interacting surfaces that are critical for dimerization and catalytic activity. This state of transient inactivity and change in dimer conformation persists until deubiquitination. The continuous association of D2 with this regulatory protein complex supports rapid cycles of deiodination, conjugation to ubiquitin, and enzyme reactivation by deubiquitination, allowing tight control of thyroid hormone action.

Thyroid hormone receptors are ligand-dependent transcription factors that can either activate or repress transcription. Deiodination is a critical process that can convert the minimally active T4 molecule to the ligand for thyroid hormone receptors, T3. While there are three known deiodinases, the type 2 iodothyronine deiodinase (D2) is the key enzyme necessary for intracellular T3 production, a process shown to be critical in development (8, 16, 24), neuroendocrine gonadal control (33), and energy homeostasis (27, 31). Given the fact that D2 catalyzes intracellular T3 production, it is not surprising that changes in D2 expression can modulate the thyroid hormone signaling pathway in a tissue-specific fashion, without affecting serum T3 concentrations (5).

The D2 pathway, and hence tissue-specific thyroid hormone signaling, is regulated by ubiquitination, a critical posttranslational regulator of protein stability (11, 25). D2 ubiquitination is accelerated in proportion to T4 concentration, thus creating a feedback loop controlling T3 production. D2 is inactivated upon conjugation to ubiquitin and, like other ubiquitinated proteins, targeted to the proteasome system (18, 29). The physiological relevance of this pathway is illustrated in the tibial growth plate of developing chickens, where ubiquitination of D2 and thus thyroid hormone signaling are under the control of the Hedgehog signaling cascade. In response to Hedgehog signaling, the D2-specific ubiquitin ligase WD repeat and SOCS box-containing 1 (WSB-1) is induced in perichondrial cells, thus accelerating D2 ubiquitination (16). The resulting decrease in D2 activity and local T3 concentration is thought to contribute to the Hedgehog induction of parathyroid hormone-related peptide (PTHrP) (16). The link between D2 activity and PTHrP has been further substantiated by studies showing that pharmacologic acceleration of D2 ubiquitination via non-Hedgehog pathways also results in induction of this peptide (16). Alternatively, ubiquitinated D2 can be reactivated by von Hippel-Lindau protein-interacting deubiquitinating enzymes 1 and 2 (VDU-1 and VDU-2, respectively), rescuing D2 from proteasomal degradation. Thus, in response to sympathetic signaling, VDU-1 is induced in brown adipocytes, accelerating D2 deubiquitination and local T3 production, playing a role in brown adipose tissue adaptive thermogenesis (14).

D2 is an endoplasmic reticulum-resident type 1 integral membrane enzyme (2, 3, 12) that exists as a homodimer as determined by nondenaturing sodium dodecyl sulfate-polyacrylamide gel electrophoresis (SDS-PAGE) and coimmunoprecipitation studies (13, 23). A current model for D2 ubiquitination consists of a ubiquitinating catalytic core complex modeled as elongin BC-Cul5-Rbx1 (ECS^{WSB-1}) assembled in close association with the D2-D2 dimer (16). In order to gain insight into the molecular mechanisms through which ECS^{WSB-1}-mediated D2 ubiquitination inactivates D2, we sought to characterize the structural determinants of the D2-D2 dimer, as well as its relationships with the ECS^{WSB-1} catalytic core complex during D2 ubiquitination and deubiquitination. Our results indicate that while ubiquitination can target the D2 protein for degradation, it also regulates D2

* Corresponding author. Mailing address: Brigham and Women's Hospital, 77 Avenue Louis Pasteur, HIM Bldg. 643, Boston, MA 02115. Phone: (617) 525-5153. Fax: (617) 731-4718. E-mail: abianco@partners.org.

† These authors contributed equally to this paper.

▽ Published ahead of print on 23 April 2007.

activity at another level by mediating a transient conformational change within the D2-D2 dimer, thus identifying a novel molecular underpinning of cell-specific thyroid hormone activation.

MATERIALS AND METHODS

Reagents. Unless otherwise specified, all reagents were obtained from Sigma (St. Louis, MO) or Calbiochem (La Jolla, CA). T4, obtained from Sigma (St. Louis, MO), was dissolved in 40 mM NaOH. Outer-ring-labeled ^{125}I-T4 (specific activity, 4,400 Ci/mmol) was from NEN Life Science Products (Boston, MA). All restriction enzymes and Vent DNA polymerase were from New England Biolabs, Inc. (Beverly, MA). Lipofectamine 2000 was from Invitrogen (Carlsbad CA), and MG132 was from Calbiochem (San Diego, CA).

DNA constructs. All DNA fragments were generated with Vent PCR on templates containing the coding region of human D2 with a Cys-mutated active center. Deiodinase fragments were fused to the carboxyl end of yellow fluorescent protein (YFP) or cyan fluorescent protein (CFP), in vector pEYFP-C1 or pECFP-C1 (Clontech), respectively, while pEYFP-N1 or pECFP-N1 was used to fuse D2 to the amino end of YFP or CFP. A similar strategy was used to fuse the N-FLAG-tagged and transmembraneless version (lacking the first 42 amino acids [aa]) of D2 to the N terminus of YFP. The D2 fragment was also fused to the N terminus of humanized *Renilla* luciferase (*R*Luc) by replacing CFP with *R*Luc in pECFP-N1. To fuse mouse WSB-1 to the N terminus of YFP, the pEYFP-N1 vector was used. The WSB-1 SOCS box from aa 242 to the C terminus was also attached to the C terminus of YFP, yielding mWSB-1–YFP-SOCS. To fuse the human VDU-1 fragment (from aa 29 to the C terminus) to the C terminus of CFP or YFP, we replaced enhanced green fluorescent protein of the pEGFPC3–hVDU-1–KpnI-ApaI construct (kindly donated by Zaibo Li) with enhanced CFP or enhanced YFP (EYFP), resulting in CFP–hVDU-1 and YFP–hVDU-1, respectively. The mouse UBC-7 was fused to the C or N terminus of YFP (using the pEYFP-C1 or pEYFP-N1 vector), resulting in YFP–mUBC-7 and mUBC-7–YFP, respectively. The mouse UBC-7 was also fused to the N terminus of CFP in pECFP-N1 by a similar strategy, resulting in mUBC-7–CFP.

Cell culture, transfections, and D2 assay. HEK-293 cells were plated in 60-mm plates and transfected using Lipofectamine 2000, and when appropriate, human growth hormone (thymidine kinase growth hormone) was used to monitor transfection efficiency (30). The amounts and types of plasmids transfected in each experiment are indicated in the respective figure legends. In most experiments, 48 h after transfection, the cells were washed twice in phosphate-buffered saline (PBS) and live-cell fluorescent resonance energy transfer (FRET) imaging was performed as detailed below. In some cases cell sonicates were prepared, D2 activity was assayed as described earlier (12) in the presence of 20 mM dithiothreitol and 1 nM ^{125}I-T4, and results were reported as fmol/min/mg protein.

FRET data and image acquisition. We used confocal microscopy-based FRET detection by acceptor photobleaching, which ensures a reduction of energy transfer when the acceptor is photobleached and an increase in the donor fluorescence (21). Numerical data were obtained and images were acquired with the use of a Zeiss LSM 510 confocal microscope (Carl Zeiss, Inc., Thornwood, NY). A 25-mW argon laser tuned to lines at 458, 477, 488, and 514 nm, with a tube current of 6.1 A, was used. Live HEK-293 cells in PBS were viewed and examined, and images were taken with an Achroplan 63- × 0.9-W water objective (2× zoom). Typically, a 2-μm optical slice was used to visualize a cell expressing the constructs of interest, tagged with CFP and YFP. Dual excitation of CFP and YFP was achieved by using an argon laser with a 458-nm/514-nm dual dichroism (21). Optimized images were collected at 12-bit resolution over 512 × 512 pixels with a pixel dwell time of 1.6 μs (20). A cell was selected as the region of interest, which was then irradiated with the 514-nm laser line (100% intensity), and the number of iterations was varied, although the goal was to photobleach YFP as quickly as possible. The general goal has been to obtain around 85% photobleaching (9) for an effective FRET. To better appreciate the occurrence of FRET, caution was taken not to saturate the region of interest. Postbleach images were acquired immediately following acceptor (YFP) photobleaching. FRET was present when YFP photobleaching yielded an increase in CFP fluorescence intensity (20). FRET efficiency was calculated by using the following equation:

$$100 \times \frac{(\text{CFP postbleach fluorescence intensity} - \text{CFP prebleach fluorescence intensity})}{\text{CFP postbleach fluorescence intensity}}$$

A minimum of at least 10 cells to a maximum of 90 cells per condition were studied. Results were calculated as a percentage of the signal measured in cells expressing a CFP-YFP positive-control fusion protein. In these positive-control cells, an approximately 20% increase in CFP fluorescence after YFP photobleaching is typically observed (data not shown).

Bioluminescence resonance energy transfer (BRET) assay. Briefly, HEK-293 cells were cultured and transfected as reported above, with the following differences: 1.5 μg each of D2-*R*luc and D2-YFP constructs was used per 60-mm plate for a single experiment. Forty-eight hours posttransfection, cells were washed twice with PBS, detached in PBS containing 2 mM EDTA, centrifuged, and resuspended in PBS containing 0.1% glucose. About 100,000 cells were dispensed into each well of a 96-well plate with clear bottoms and back walls to minimize noise caused by autofluorescence. Studies in cell sonicates were done by resuspending the cell pellet in 250 μl of PBS containing 0.1% glucose followed by brief sonication. Protein was measured by the Bio-Rad protein assay, and equal amounts of protein were added to each well.

To activate *R*Luc, 1× of its substrate (coelenterazine) was diluted in the same buffer and read after 10 s in a Fluostar Optima fluorimeter (BMG Lab Technologies, Offenburg, Germany), programmed with the appropriate software and filters: 475 to 30 nm for *R*Luc and 535 to 30 nm for YFP at a preset gain. BRET ratios were calculated using the following formula:

$$\frac{(\text{YFP emission at 535 to 30 nm})}{R\text{Luc (475 to 30 nm)}} - R\text{Luc (475 to 300 nm)}^*$$

The asterisk marks the sample where the *R*Luc construct is expressed alone.

Sequence analysis and structure modeling. Further sequence analysis of the deiodinase iduronidase-like insertion has been conducted using hydrophobic cluster analysis (7, 17), as previously reported for the construction of the thioredoxin fold model of deiodinases (6) or for the structural insights devoted to the D2 ubiquitin ligase (16). Three-dimensional (3D) models were built and handled using the Swiss PDB viewer tool (19).

RESULTS

D2 dimerization surfaces exist in the transmembrane and globular domains. When transiently expressed in HEK-293 cells, D2-CFP and D2-YFP display endoplasmic reticulum distribution (Fig. 1A), as seen in endogenous expression (12, 16, 18, 22). The YFP photobleaching approach to measuring FRET revealed that the D2-D2 FRET signal reached about 75% of that detected in positive-control cells expressing a well-characterized CFP-YFP fusion protein with a high degree of FRET (10) (Fig. 1B and data not shown), and no significant energy transfer was observed in cells expressing CFP, YFP, or both (Fig. 1B). D2-D2 FRET was detected regardless of whether both chromophores were fused to the amino or to the carboxyl end of D2 (Fig. 1B), but FRET was absent if the chromophores were placed in opposite orientations (Fig. 1B). This specificity was confirmed when D2-D2 dimerization was monitored by an alternative approach that used BRET (Fig. 1B and data not shown) in cells expressing D2 fused to *R*Luc and D2-YFP. Coexpression of D2 with the structurally related D1 enzyme fused to the appropriate chromophores did not result in measurable energy transfer by FRET or BRET (data not shown).

We next sought to characterize the structural basis of the D2-D2 dimer interaction. The single D2 transmembrane segment starts near C22 and ends near L41 (Fig. 1C). This is a typical transmembrane helix containing potentially charged residues (D, E, K, and R as well as H) that would normally achieve stability in the hydrophobic membrane environment by dimerization. In this way, charged residues could be neutralized via intermolecular interaction of residue couples such as D29/K35 as well as direct contacts between polar residues such as H36-K35′, compatible with modeling of the two D2 transmembrane segments in an α-α dimeric architecture (data not shown). To study the role of this segment in D2-D2 dimeriza-

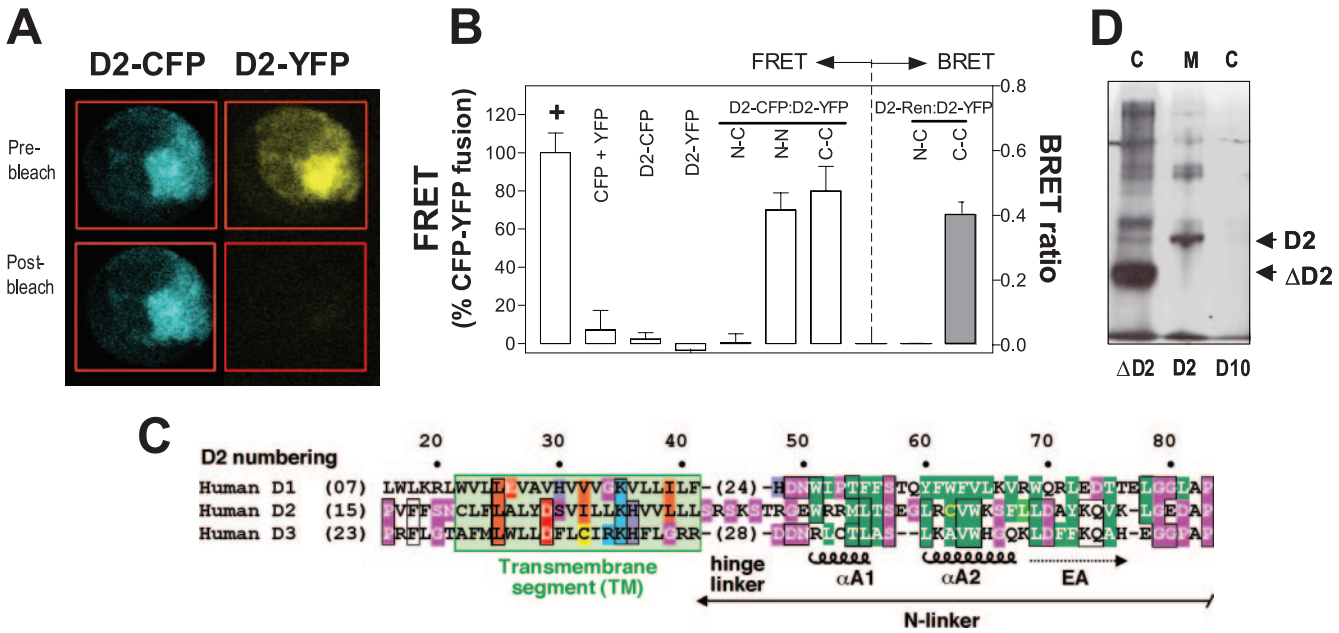

FIG. 1. D2 holoenzyme is a homodimer. (A) Photomicrography of an individual HEK-293 cell transiently coexpressing D2-CFP and D2-YFP, pre- and post-YFP photobleaching. (B) Quantification of D2-D2 FRET in cells expressing D2-CFP and/or D2-YFP fused at the indicated termini of D2. The location of the chromophores in the D2 molecule is indicated by N (amino) or C (carboxyl) for CFP and YFP, respectively. Results were calculated as a percentage of the signal measured in cells expressing a CFP-YFP positive-control (+) fusion protein. In these positive-control cells, an approximately 20% increase in CFP fluorescence after YFP photobleaching is typically observed (data not shown). Also shown (right axis) is the D2-D2 BRET ratio in cells expressing D2-*R*Luc and D2-YFP. The location of the chromophores in the D2 molecule is indicated by N (amino) or C (carboxyl) for YFP and *R*Luc, respectively. Data are means ± standard deviations of at least 10 data points. (C) Partial sequence alignment of human D1, D2, and D3, denoting the transmembrane and N-linker regions (6). Hydrophobic residues are green, loop-forming residues are depicted by white letters on a pink background, and the neutral amino acid H is shown on a purple background; the putative transmembrane segment (20 aa) is shown on a light green background, with amino acids likely to be in tight contact in the dimer interface shown in orange. Red, acidic; blue, basic; yellow, cysteine. (D) Western blot analysis with anti-FLAG antibody of cytosol (C) or microsomal (M) subcellular fractions of cells transiently expressing a truncated D2 without the transmembrane domain (ΔD2), full-length D2 (D2), or empty D10 vector.

tion, a truncated D2 molecule missing the first 42 aa (ΔD2) was expressed and found to be a cytosolic protein (Fig. 1D) that does not homodimerize (Fig. 2A). While this indicates a critical role for the transmembrane domain in dimerization, it does not exclude a possible role of the globular domain as well. In fact, coexpressing ΔD2-YFP and a full-length D2-CFP molecule produced about 60% of the FRET detected in the full-length D2-D2 dimer (Fig. 2A), and this occurred only if the chromophores were fused to the C termini of the two molecules, confirming that the interaction is through the globular domain (Fig. 2A). Based on these data, we sought to characterize the D2 globular dimerization interface. Since D2 is known to be a thioredoxin fold-containing protein (6), this interface was tentatively modeled by comparison to the human thioredoxin fold, which shows a clear propensity to dimerize via a large interface formed by the alignment of two β strands that constitute a small β sheet (32). Due to the high sequence identity around the canonical thioredoxin β1α2β2 motif, the D2 globular dimerization model could be fitted on the crystal structure of dimeric oxidized thioredoxin (PDB identifier 1eru) with no evident clash (Fig. 2C). In subsequent studies we failed to identify additional potential dimerization interfaces in the long and well-conserved segment S42 to K76, which connects the transmembrane and globular domains of D2, modeled as a miniglobule with all hydrophobic amino acids clustered into an internal core (Fig. 2D). Taken as a whole, these studies suggest that the native D2-D2 dimer is formed by interactions at both the transmembrane and the globular domains (Fig. 2D). This model reveals a region of negative electrostatic potential around the active sites that could act as an attracting field for the hormone and a large positive region for the rest of the molecules (Fig. 2E).

Ubiquitination transiently induces a conformational change within the D2-D2 dimer. Having established the dimeric nature of the D2 molecule, we next wished to investigate the role of dimerization in enzymatic activity. In initial studies using increasing concentrations of urea to promote conformational changes in the D2-D2 dimer, we observed a correlation between loss of BRET signal and enzymatic activity (data not shown). Taking advantage of the ΔD2-D2 dimerization (Fig. 2A), we looked at how dimerization affects enzyme activity by coexpressing a full-length catalytically inactive D2 molecule (with Ala replacing the critical selenocysteine [Sec] residue in the active center of the enzyme [Ala133D2]) with the Sec-containing ΔD2. While the Sec-containing ΔD2 molecule is inactive when expressed alone (Fig. 2B), when it is expressed in combination with Ala133D2, D2 catalytic activity is readily measurable (Fig. 2B). This indicates that dimerization of the globular domains is sufficient for D2 catalytic activity. The fit between ΔD2 and Ala133D2 molecules seems to position the

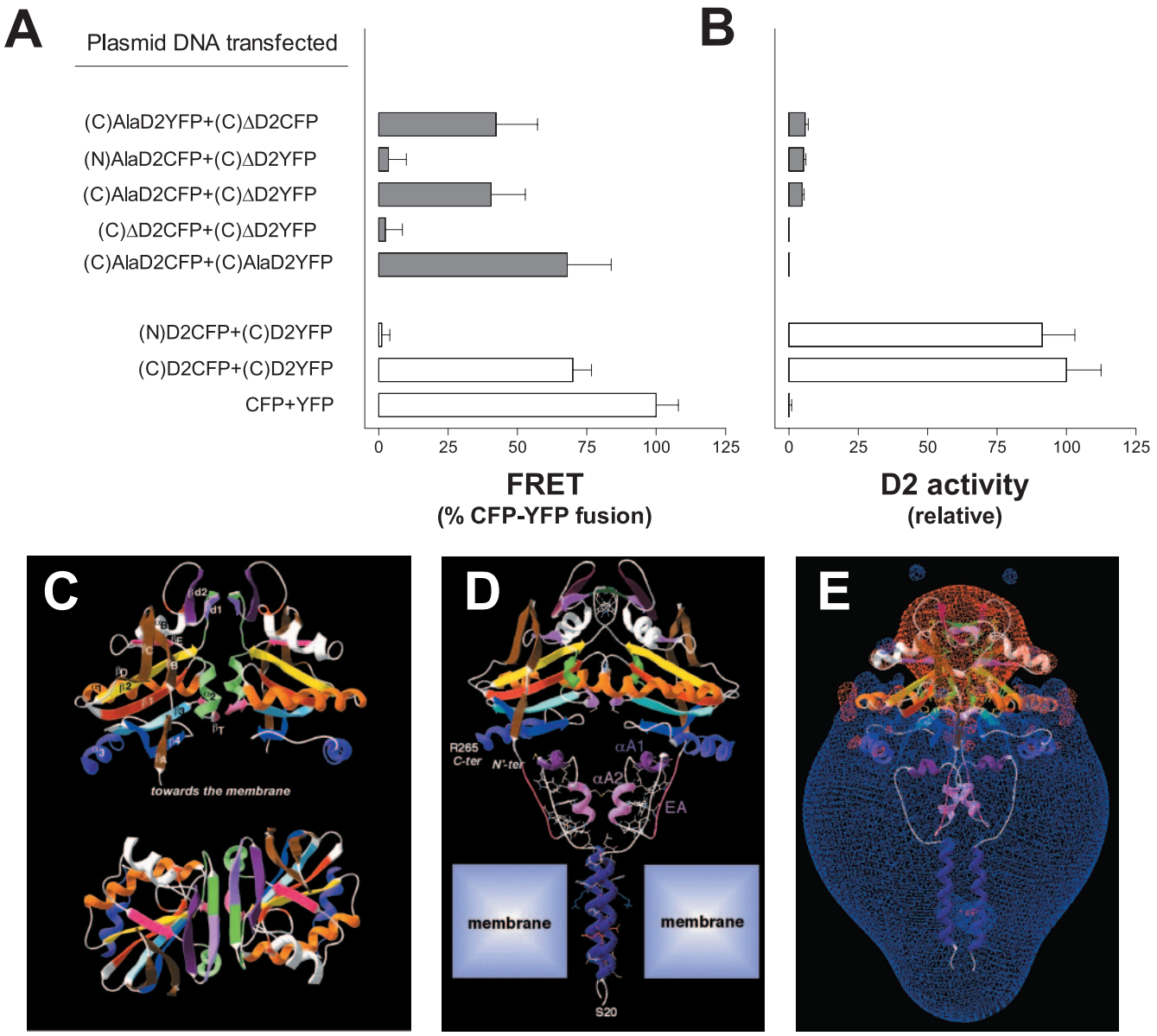

FIG. 2. Globular interfaces mediate D2 dimerization and are critical for catalytic activity. (A) FRET signal in cells expressing the indicated D2 proteins fused to either CFP or YFP at the amino (N) or carboxyl (C) termini of the D2 molecule. AlaD2 is a full-length D2 molecule in which Sec133 was mutated to Ala. (B) D2 activity in cell sonicates shown in panel A. In panels A and B, data are means ± standard deviations of at least 10 data points. (C) Two orthogonal views of the modeled D2 dimer on the template of the crystal structure of human thioredoxin dimer. At the top, the twofold axis is vertical, and at the bottom, it is perpendicular to the figure. Secondary structures are colored as published elsewhere (6) and labeled accordingly. The putative structure of the iduronidase-like active site insertion has been modeled as a ββ secondary structure (βd1 and βd2) lying between β2 and αB. βd1 is colored green/light purple, βd2 is in in dark purple, and at the bottom of the dimer, the two symmetrical small βT structures (D2 G224, V225, A226; pink) are the counterparts of the canonical thioredoxin pairing. (D) 3D model of the D2-D2 dimer. N′-ter and C-ter indicate the N terminus of the thioredoxin fold head domain and the C terminus of D2, respectively. The S42-K76 connecting segment is rich in strongly hydrophobic amino acids (VILFMYW), which are shown in atomic detail. The N and C termini of this segment readily match the C and N termini of the transmembrane and globular domains, respectively. The buried dimeric interface for the full model is 2,170 Å^2 (in the range observed for moderately strong dimers and slightly higher than those of many protein complexes [1]), that for the head is 1,343 Å^2 (more than twice that for the thioredoxin dimer), that for the N-linker is 128 Å^2, and that for the transmembrane segment is 705 Å^2, confirming the respective roles of each part, particularly that of the transmembrane segments. A single large cavity (427 Å^2) is created upon D2 dimerization at the level of the active site (Sec133), which is surrounded by S130, T132, Se133, P134, I161, D162, M215, N218, Y223, G224, V255, A226, E228, and their symmetric residues. (E) Visualization of the Russian-doll-shaped electrostatic field around the D2 dimer (the −1.8-kT/e gradient limit is colored red and the +1.8-kT/e gradient limit is blue).

active center in ΔD2 in its natural conformation, as the apparent enzyme K_m of T4 is indistinguishable from that of wild-type D2 protein (data not shown). However, the fact that in cells coexpressing ΔD2-Ala133D2 the FRET signal is not different from that of control cells [(C)D2CFP+(C)D2YFP] while the D2 activity is markedly reduced suggests that the transmembrane domain could modulate catalytic activity.

Based on the relationship between dimerization and D2 enzymatic activity, we asked whether ubiquitin-mediated enzyme inactivation induced by exposure to T4 (18) could be a

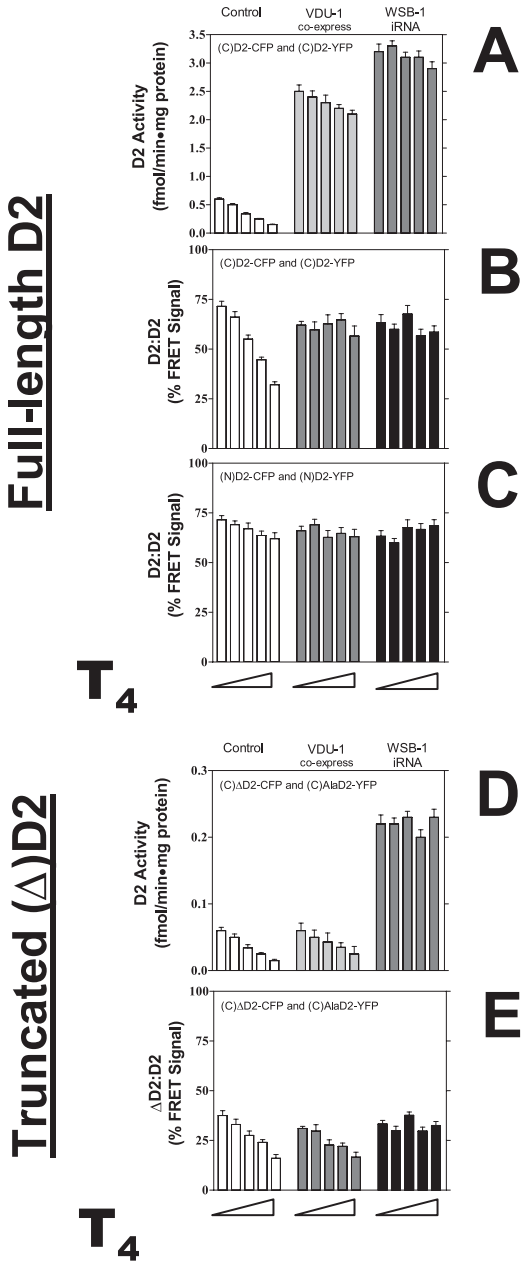

FIG. 3. Properties of D2-D2 dimer during catalysis. In all experiments cells were treated with 0, 0.1, 1, 5, or 10 μM T4 (from left to right) in 10% charcoal-stripped fetal bovine serum-containing medium for 4 h immediately prior to harvesting or FRET studies. (A) D2 activity in cells coexpressing full-length D2-CFP and D2-YFP; chromophores were placed at the carboxyl (C) terminus of D2; VDU-1 or WSB-1 interfering RNA (iRNA) plasmids were also used as indicated. (B) D2-D2 FRET signal in cells transfected as in panel A. (C) D2-D2 FRET signal in cells coexpressing D2-CFP and D2-YFP; chromophores were placed at the amino (N) terminus of D2. (D) Same as in panel A, except that ΔD2 was used. (E) ΔD2-D2 FRET signal in cells transfected as in panel D. Data are means ± standard deviations of at least 10 data points.

product of conformational changes within the D2-D2 dimer. This was tested by exposing D2-expressing cells to progressively higher concentrations of T4 (Fig. 3A to E). Initially we looked at FRET between the globular domains using D2 molecules containing chromophores fused to the carboxyl ends. Remarkably, exposure to T4 resulted in progressive loss of globular FRET signal in the D2-D2 dimer (Fig. 3B). This is presumably due to T4-induced ubiquitination and not overall loss of D2 protein, since the FRET signal being monitored is the fractional increase in CFP intensity after 90 seconds of YFP photobleaching. To test this hypothesis, similar studies were performed using small interfering RNA for WSB-1, under conditions that we have shown elsewhere to knock down WSB-1 expression and prevent D2 ubiquitination (16) (data not shown). Under these conditions, exposure to increasing concentrations of T4 only minimally inactivated D2 (Fig. 3A) and failed to promote the conformational change within the D2-D2 dimer (Fig. 3B), further suggesting that conjugation to ubiquitin interferes with the D2 globular dimerization interface. The T4-mediated dimer conformational change was the same in cells treated with the proteasome inhibitor MG132 (data not shown), indicating that this is not mediated by the proteasomes.

Next, we sought to determine whether these ubiquitination-induced changes in the D2-D2 dimer are reversible or lead to a terminal disassembly of the D2 holoenzyme. This was studied by coexpressing the D2-specific deubiquitinase VDU-1 (14). Under these conditions, exposure to increasing concentrations of T4 did not result in loss of D2 activity (Fig. 3A) or conformational changes within the D2-D2 dimer (Fig. 3B). These data support the reversibility of these T4-induced changes in D2-D2 dimer conformation-caused ubiquitination. The transient nature of this D2-D2 dimer interference suggests that other interacting surfaces in the dimer are also preventing its irreversible disassembly. To test this possibility, FRET studies were repeated using D2 molecules containing chromophores fused to their amino ends (Fig. 3C). Remarkably, from this perspective, ubiquitin-mediated conformational change within the D2-D2 dimer was almost nonexistent, indicating that the transmembrane-interacting surfaces remain largely unaffected during the ubiquitination/deubiquitination cycle. This model is further supported by the findings that the T4-induced changes within the ΔD2-D2 dimer are irreversible, given that normal dimerization cannot be reestablished by accelerating D2 deubiquitination with VDU-1 coexpression (Fig. 3D and E). Only WSB-1 knockdown can prevent such changes in the ΔD2-D2 dimer (Fig. 3D and E). Taken together, these studies indicate that T4-induced D2 ubiquitination promotes a conformational change within the globular domains, while the transmembrane domains remain largely unaffected by ubiquitin conjugation.

The ECS^{WSB-1} catalytic core complex is continuously assembled around D2. In the next set of experiments, we wished to evaluate the relationships of the D2-D2 dimer with the ECS^{WSB-1} catalytic core complex and VDU-1, a D2-specific deubiquitinase. This was done by coexpressing appropriate chromophore-labeled D2, WSB-1, UBC-7, and/or VDU-1. A strong FRET signal, equivalent to that of the D2-D2 dimer, was obtained from D2 interactions with WSB-1, UBC-7, and VDU-1. Remarkably, significant energy transfer was detected even when D2 ubiquitination was minimized, i.e., in the absence of T4, suggesting a continuous association between ECS^{WSB-1} catalytic core complex and D2 (Fig. 4A and B). Coexpression studies indicate that each of these D2-interacting proteins attaches to distinct and

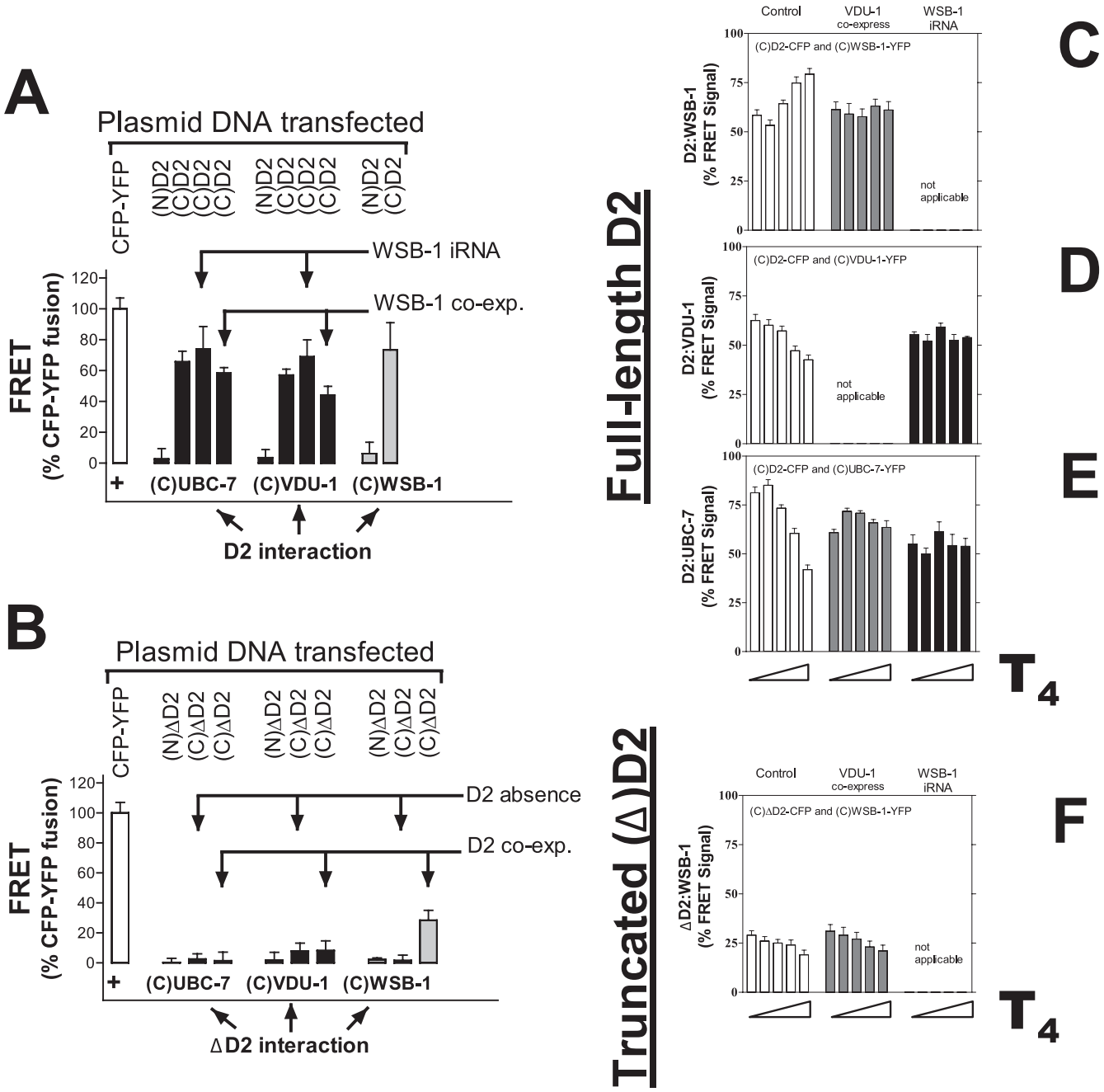

FIG. 4. D2 interaction with UBC-7, WSB-1, and VDU-1. (A) FRET studies in HEK-293 cells transiently coexpressing D2-CFP and UBC-7–YFP, WSB-1–YFP, or VDU-1–YFP. As indicated, some studies were performed in cells with WSB-1 knockdown (interfering RNA [iRNA]) or coexpressing WSB-1. The positions of the chromophores in the D2 molecule are indicated as amino (N) or carboxyl (C) termini. (B) Same as panel A, except that the interactions of ΔD2 with UBC-7, VDU-1, or WSB-1 were studied in the absence of or during full-length D2 coexpression. In the experiments for panels C to F cells were treated with 0, 0.1, 1, 5, or 10 μM T4 (from left to right) in 10% charcoal-stripped fetal bovine serum-containing medium for 4 h immediately prior to FRET studies. (C to E) D2 interaction with WSB-1 (C), with VDU-1 (D), and with UBC-7 (E), with or without VDU-1 or WSB-1. (F) Same as in panel C, except that ΔD2 was used. Data are means ± standard deviations of at least 10 data points.

independent interactive surfaces on the D2-D2 dimer, as WSB-1 knockdown or coexpression only minimally interfered with D2–UBC-7 or D2–VDU-1 interactions (Fig. 4A). Additionally, coexpression of UBC-7 and VDU-1 did not interfere with either protein's interaction with D2 or with the D2–WSB-1 interaction (data not shown). Cross-binding and dimerization were minimal and observed only between WSB-1 and UBC-7 and between UBC-7 and UBC-7, respectively, and both were disrupted by D2 coexpression (data not shown). While we cannot exclude the possibility that the ECS^{WSB-1} catalytic core complex interacts with D2 as a monomer, ΔD2 did not interact with WSB-1 except when

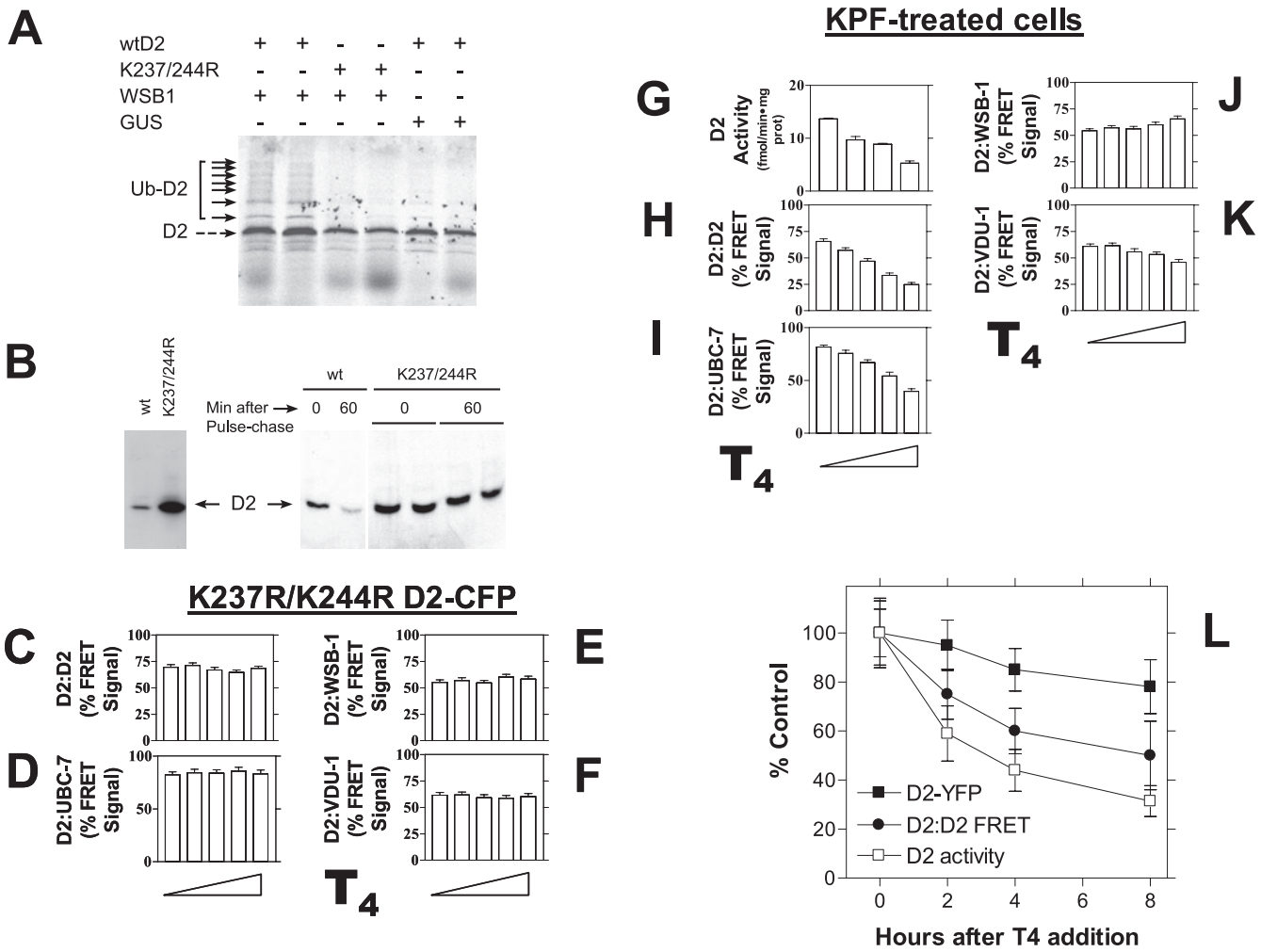

FIG. 5. Mechanism of D2 ubiquitination. (A) A ^{35}S-labeled D2 or K237R/K244R D2 mutant was used in the in vitro ubiquination assay in a reticulocyte lysate system containing 10 μM ubiquitin aldehyde, energy solution, and 30 μM ubiquitin as previously described (16). Bacterially expressed WSB-1 or *Arabidopsis thaliana* β-glucoronidase (GUS) was added as indicated after normalization by Coomassie blue stain SDS-PAGE. Ubiquitinated D2 was immunoprecipitated using D2 antiserum (IP α-D2), and the pellets were resolved by SDS-PAGE. The black arrows indicate the ubiquitin–^{35}S-D2 conjugates (Ub-^{35}S-D2). wt, wild type. (B) Immunoprecipitation of ^{35}S-labeled D2 or K237R/K244R D2 mutant using anti-FLAG after a 60-min pulse-chase. In the experiments shown in panels C to F and H to K, cells were treated with 0, 0.1, 1, 5, or 10 μM T4 (from left to right) in 10% charcoal-stripped fetal bovine serum-containing medium for 4 h immediately prior to harvesting or FRET studies. (C to F) K237R/K244R D2-CFP mutant was used. FRET signals in cells expressing the indicated proteins are shown: D2-D2 (C), D2–UBC-7 (D), D2–WSB-1 (E), and D2–VDU-1 (F). (G and H) D2 activity (G) and D2-D2 FRET signal (H) in cells coexpressing full-length D2-CFP and D2-YFP and pretreated with 40 μM kaempferol (KPF) for 12 h. For D2 activity (G), treatments were 0, 0.1, 1, or 5 mM T4. (I to K) Under similar conditions the FRET signals between D2 and UBC-7 (I), D2 and WSB-1 (J), and D2 and VDU-1 (K) were also obtained. (L) Same as in panels G and H except that cells were treated with 10 μM T4 for the indicated times and D2-YFP signal was also measured. Data are means ± standard deviations of at least 10 data points.

full-length D2 was simultaneously coexpressed (Fig. 4B), indicating that WSB-1 binds the D2-D2 dimer. This also indicates that the N linker and/or the globular domains in D2 are sufficient to mediate WSB-1 recognition. UBC-7, on the other hand, did not bind to ΔD2 under any circumstance, and VDU-1 binding to ΔD2 was minimal and not affected by full-length D2 coexpression (Fig. 4B). The latter also provides an alternate explanation as to why VDU-1 coexpression failed to rescue the loss of ΔD2-D2 dimerization upon exposure to T4 (Fig. 3D and E).

The finding of an association between D2 and UBC-7 independent of WSB-1 is notable. As the cullin/Rbx1 heterodimer is generally believed to recruit E2s for ubiquitination (34), knockdown of WSB-1 would intuitively be expected to disrupt the interaction between D2 and UBC-7, but this was not the case (Fig. 4A). In fact, we have previously shown that human D2 specifically associates with UBC-7 (but not UBC-6) in reticulocyte lysates as well as when it is transiently expressed in HEK-293 cells, with localization to aa 169 to 234 of D2, independent of WSB-1 (22). These data are consistent with our present results and also suggest a possible role played by UBC-7 in ECS^{WSB-1} assembly.

Given that exposure to T4 promotes D2 ubiquitination and a marked conformational change in the D2-D2 dimer, our next

question was whether such effects could modulate D2 interaction with the key proteins in the ECS^{WSB-1} catalytic core complex or VDU-1 (Fig. 4C to F). Notably, exposure to T4 increased the D2–WSB-1 association while decreasing the interactions of D2–VDU-1 and D2–UBC-7 (Fig. 4C to E). These changes are likely to result from D2 ubiquitination, given that they are minimized with coexpression of VDU-1 or by WSB-1 knockdown. However, our studies do not address the timing with which these changes occur. Thus, it is difficult to speculate whether the conformational change within the D2-D2 dimer is a cause or result of such changes or whether after ubiquitination WSB-1 could occupy VDU-1 or UBC-7 binding sites in the D2-D2 dimer. In contrast, the association between the ΔD2-D2 dimer and WSB-1 does not increase with exposure to T4 (Fig. 4F), suggesting that perhaps the ΔD2-D2 dimer is terminally disassembled upon ubiquitination.

Human D2 contains 15 Lys residues. To identify which one is ubiquitinated by the ECS^{WSB-1} catalytic core complex, 13 Lys residues were replaced with Arg in different combinations, while the carboxyl-terminal 267KK268 pair was truncated. After extensive analysis, a combined K237R/K244R catalytically inactive D2 mutant was identified as being resistant to WSB-1-mediated ubiquitination in vitro (Fig. 5A). In fact, based on our D2-D2 model (Fig. 2C to E), K244 lies within the dimer interface, near the Sec residue of the catalytic site, and its ubiquitination would be expected to interfere with the D2-D2 conformation. In addition, K237 is in the vicinity of K244, within the hinge area between the thioredoxin-folded domain and the N-linker small domain, and thus also in a position to affect overall dimer stability. When expressed in cells, the K237R/K244R D2 mutant remained in the endoplasmic reticulum (data not shown) but accumulated about fivefold above wild-type levels as a result of having a much longer half-life in [^{35}S]methionine metabolic labeling studies (Fig. 5B). Interestingly, the isolated K237R or K244R D2 mutants is active and behaves normally in all aspects studied (data not shown), suggesting that WSB-1-mediated D2 ubiquitination can take place in either one of these residues. In subsequent studies, the K237R/K244R D2 mutant was found to be a dimer that, unlike the wild-type molecule, is stable upon exposure to T4 (Fig. 5C). Exposure to T4 also failed to change the interaction between the double Lys mutant and UBC-7, VDU-1, or WSB-1, indicating that these processes depend on conjugation to ubiquitin (Fig. 5C).

It has already been established that T4 must interact with the Sec residue in the D2 active center in order to increase D2 susceptibility to ubiquitination (28), but it is not known whether catalysis, i.e., T3 production, is necessary. To address this question, D2-expressing cells were treated with kaempferol, a flavonol that at 40 μM specifically prevents D2-mediated T4-to-T3 conversion by interfering with the endogenous cofactor for D2 (Fig. 3A) (15). In control cells, exposure to increasing concentrations of T4 resulted in T3 production (up to 1.0 fmol T3/h/mg protein) and ~50% loss of D2 activity due to ubiquitination (Fig. 5G). At the same time, in kaempferol-treated cells, exposure to T4 was associated with only minimal T3 production (up to 0.05 fmol/h/mg protein) but the loss in D2 activity was similar (Fig. 5G). Thus, in the absence of substantial T4 catalysis, the same D2-D2 modifications were observed as when T3 is produced, i.e., loss of D2 catalytic activity (Fig. 5G) and of changes in D2-D2 dimer conformation (Fig. 5H), as well as a decrease in the D2–UBC-7 and D2–VDU-1 associations and an increase in D2–WSB-1 association (Fig. 5I to K). These data indicate that binding of T4 to the D2 active center is sufficient to trigger D2 ubiquitination, presumably by inducing conformational changes within the D2-D2 dimer that result in exposure of the critical K237R/K244R to UBC-7.

Lastly, we evaluated the relative contributions of changes in dimer conformation versus D2 proteolysis to the overall loss of D2 activity during exposure to T4. Monitoring D2-YFP signal as an index of intracellular D2 levels in parallel with D2 activity and D2-D2 FRET signal in live cells addressed this question. Upon exposure to T4, there was a rapid and progressive loss in D2 activity that was predominantly due to the modification within the D2-D2 dimer. At the same time, D2 degradation as assessed by loss of D2-YFP signal contributed much less to the loss in D2 activity (Fig. 5L).

DISCUSSION

The data obtained in the present studies describe details of the mechanism through which conjugation to ubiquitin can regulate deiodinase function and thyroid hormone activation. Our model system is based on an integral membrane protein that exhibits catalytic activity only in a dimeric conformation (Fig. 1 and 2). In this system, substrate-induced ubiquitination inactivates the D2 enzyme by transiently interfering with its dimeric conformation (Fig. 3). While the FRET and BRET studies were performed in cells transiently expressing the different D2 fusion proteins, the intrinsic properties of these proteins such as subcellular localization, turnover rate, and responsiveness to T4, D2's natural substrate, are indistinguishable from those of endogenous D2 (12). Under these conditions, it is intriguing that the WSB-1- and VDU-1-based catalytic core complex that regulates D2-D2 ubiquitination is continuously associated with dimeric D2 (Fig. 4), instead of being assembled at every cycle of deiodination, ubiquitination, and deubiquitination.

The picture that emerges from the present study is that D2 has two dimerization surfaces: one involves its transmembrane domain while the other involves its globular catalytic domain. In addition, it is clear that globular homodimerization is sufficient for catalytic activity (Fig. 2A and B). As ΔD2 is inactive and does not homodimerize (i.e., ΔD2-ΔD2 [Fig. 2A and B]), the interaction between these two truncated molecules containing only the globular domain does not mediate stable dimerization. However, ΔD2 still dimerizes with full-length D2, which results in catalytic activity (Fig. 2A and B). While it is unclear why there is no interaction between two ΔD2 globular domains in the cytosol, the finding that ΔD2-D2 globular domains do dimerize indicates that insertion in the endoplasmic reticulum membrane of at least one of the dimer counterparts is required to accommodate globular dimerization.

FRET decreases as the physical distance between the chromophores increases. Thus, one interpretation of the T4-induced loss of D2-D2 FRET signal is that ubiquitination promotes a change within the D2-D2 dimer that increases the physical separation of the two chromophores. WSB-1-mediated D2 ubiquitination takes place at K237 and/or K244 (Fig. 5).

Given that K244 lies within the dimer interface near the Sec residue of the catalytic site (6), its ubiquitination and/or that of its neighbor K237 provides a possible molecular mechanism for such conformational change to occur. Regardless of the mechanism, it is remarkable that such interference with the D2-D2 dimer is restricted to the globular domain of the enzyme, which contains the active center, but does not affect the transmembrane domains (Fig. 3). This sets the stage for a mechanism in which deubiquitination restores D2 catalytic activity by reversing ubiquitin-mediated change in D2-D2 dimer conformation.

The fact that pharmacological inhibitors of the proteasome prolong D2 half-life (28, 29) suggests that some D2 is eventually degraded through this system, although it is not clear what determines the fate of ubiquitinated D2. The fact that the D2-D2 dimer is continuously associated with WSB-1, UBC-7, and VDU-1, even under conditions of minimal D2 ubiquitination (Fig. 4), suggests that D2 molecules can undergo multiple cycles of ubiquitination and deubiquitination before proteasomal degradation. This view is supported by the finding that the loss in D2 activity caused by T4 is predominantly due to conformational changes within the dimer, while proteasomal degradation contributes to a lesser extent (Fig. 5L). In fact, the constant association between D2 and these proteins contrasts with the situation for most proteins, in which modifications such as phosphorylation trigger binding to the ubiquitin ligase adaptor and the assembly of the catalytic core complex.

The sensitivity to the proteasome inhibitors could also be interpreted as supporting the existence of an alternative pathway for D2 ubiquitination. The observation that D2 accumulates in a *doa10*Δ yeast strain indicates that D2 might also be the target of the more general degradation process based in the endoplasmic reticulum, traditionally known to be associated with the proteasome (26). If this is also the case in vertebrates, an interesting possibility is that D2 would be dually regulated, first via the Hedgehog signaling pathway via the ECS^{WSB-1} catalytic core complex in which deubiquitination is possible and second via TEB4, the mammalian ortholog of *doa10*, targeting it for proteasomal degradation.

D2 contains the rare amino acid Sec in its active center. Decoding the Sec-encoding UGA codon as a signal for cotranslational insertion of Sec, not termination, decreases translation efficiency 20- to 400-fold (4). Thus, due to this intrinsic inefficiency of the selenoprotein synthesis, the availability of a reversible ubiquitination-dependent mechanism to control the activity of D2 constitutes a biochemical and physiological advantage that allows for an additional control of thyroid hormone activation.

ACKNOWLEDGMENTS

We thank the optical imaging facility at the Harvard Center for Neurodegeneration and Repair, Harvard Medical School. The technical suggestions of Michelle Ocana and Mark Chafel have been helpful during this investigation.

This work was supported by grants DK58538, TW006467, and OTKA T049081.

REFERENCES

1. **Bahadur, R. P., P. Chakrabarti, F. Rodier, and J. Janin.** 2004. A dissection of specific and non-specific protein-protein interfaces. J. Mol. Biol. **336:**943–955.
2. **Baqui, M., D. Botero, B. Gereben, C. Curcio, J. W. Harney, D. Salvatore, K. Sorimachi, P. R. Larsen, and A. C. Bianco.** 2002. Human type 3 iodothyronine selenodeiodinase is located in the plasma membrane and undergoes rapid internalization to endosomes. J. Biol. Chem. **4:**4.
3. **Baqui, M. M., B. Gereben, J. W. Harney, P. R. Larsen, and A. C. Bianco.** 2000. Distinct subcellular localization of transiently expressed types 1 and 2 iodothyronine deiodinases as determined by immunofluorescence confocal microscopy. Endocrinology **141:**4309–4312.
4. **Berry, M. J., A. L. Maia, J. D. Kieffer, J. W. Harney, and P. R. Larsen.** 1992. Substitution of cysteine for selenocysteine in type I iodothyronine deiodinase reduces the catalytic efficiency of the protein but enhances its translation. Endocrinology **131:**1848–1852.
5. **Bianco, A. C., and B. W. Kim.** 2006. Deiodinases: implications of the local control of thyroid hormone action. J. Clin. Investig. **116:**2571–2579.
6. **Callebaut, I., C. Curcio-Morelli, J. P. Mornon, B. Gereben, C. Buettner, S. Huang, B. Castro, T. L. Fonseca, J. W. Harney, P. R. Larsen, and A. C. Bianco.** 2003. The iodothyronine selenodeiodinases are thioredoxin-fold family proteins containing a glycoside hydrolase-clan GH-A-like structure. J. Biol. Chem. **278:**36887–36896.
7. **Callebaut, I., G. Labesse, P. Durand, A. Poupon, L. Canard, J. Chomilier, B. Henrissat, and J. P. Mornon.** 1997. Deciphering protein sequence information through hydrophobic cluster analysis (HCA): current status and perspectives. Cell. Mol. Life Sci. **53:**621–645.
8. **Campos-Barros, A., L. L. Amma, J. S. Faris, R. Shailam, M. W. Kelley, and D. Forrest.** 2000. Type 2 iodothyronine deiodinase expression in the cochlea before the onset of hearing. Proc. Natl. Acad. Sci. USA **97:**1287–1292.
9. **Centonze, V. E., B. A. Firulli, and A. B. Firulli.** 2004. Fluorescence resonance energy transfer (FRET) as a method to calculate the dimerization strength of basic helix-loop-helix (bHLH) proteins. Biol. Proced. Online **6:**78–82.
10. **Cicchetti, G., M. Biernacki, J. Farquharson, and P. G. Allen.** 2004. A ratiometric expressible FRET sensor for phosphoinositides displays a signal change in highly dynamic membrane structures in fibroblasts. Biochemistry **43:**1939–1949.
11. **Ciechanover, A.** 2005. Proteolysis: from the lysosome to ubiquitin and the proteasome. Nat. Rev. Mol. Cell Biol. **6:**79–87.
12. **Curcio, C., M. M. A. Baqui, D. Salvatore, B. H. Rihn, S. Mohr, J. W. Harney, P. R. Larsen, and A. C. Bianco.** 2001. The human type 2 iodothyronine deiodinase is a selenoprotein highly expressed in a mesothelioma cell line. J. Biol. Chem. **276:**30183–30187.
13. **Curcio-Morelli, C., B. Gereben, A. M. Zavacki, B. W. Kim, S. Huang, J. W. Harney, P. R. Larsen, and A. C. Bianco.** 2003. In vivo dimerization of types 1, 2, and 3 iodothyronine selenodeiodinases. Endocrinology **144:**3438–3443.
14. **Curcio-Morelli, C., A. M. Zavacki, M. Christofollete, B. Gereben, B. C. G. Freitas, J. W. Harney, Z. Li, G. Wu, and A. C. Bianco.** 2003. Deubiquitination of type 2 iodothyronine deiodinase by pVHL-interacting deubiquitinating enzymes regulates thyroid hormone activation. J. Clin. Investig. **112:**189–196.
15. **da Silva, W. S., J. W. Harney, B. Kim, J. Li, S. D. Bianco, A. Crescenzi, M. A. Christoffolete, S. A. Huang, and A. C. Bianco.** 2007. The small polyphenolic molecule kaempferol increases cellular energy expenditure and thyroid hormone activation. Diabetes **56:**767–776.
16. **Dentice, M., A. Bandyopadhyay, B. Gereben, I. Callebaut, M. A. Christoffolete, B. W. Kim, S. Nissim, J. P. Mornon, A. M. Zavacki, A. Zeold, L. P. Capelo, C. Curcio-Morelli, R. Ribeiro, J. W. Harney, C. J. Tabin, and A. C. Bianco.** 2005. The Hedgehog-inducible ubiquitin ligase subunit WSB-1 modulates thyroid hormone activation and PTHrP secretion in the developing growth plate. Nat. Cell Biol. **7:**698–705.
17. **Gaboriaud, C., V. Bissery, T. Benchetrit, and J. P. Mornon.** 1987. Hydrophobic cluster analysis: an efficient new way to compare and analyse amino acid sequences. FEBS Lett. **224:**149–155.
18. **Gereben, B., C. Goncalves, J. W. Harney, P. R. Larsen, and A. C. Bianco.** 2000. Selective proteolysis of human type 2 deiodinase: a novel ubiquitin-proteasomal mediated mechanism for regulation of hormone activation. Mol. Endocrinol. **14:**1697–1708.
19. **Guex, N., and M. C. Peitsch.** 1997. SWISS-MODEL and the Swiss-PdbViewer: an environment for comparative protein modeling. Electrophoresis **18:**2714–2723.
20. **Herrick-Davis, K., E. Grinde, and J. E. Mazurkiewicz.** 2004. Biochemical and biophysical characterization of serotonin 5-HT2C receptor homodimers on the plasma membrane of living cells. Biochemistry **43:**13963–13971.
21. **Karpova, T. S., C. T. Baumann, L. He, X. Wu, A. Grammer, P. Lipsky, G. L. Hager, and J. G. McNally.** 2003. Fluorescence resonance energy transfer from cyan to yellow fluorescent protein detected by acceptor photobleaching using confocal microscopy and a single laser. J. Microsc. **209:**56–70.
22. **Kim, B. W., A. M. Zavacki, C. Curcio-Morelli, M. Dentice, J. W. Harney, P. R. Larsen, and A. C. Bianco.** 2003. ER-associated degradation of the human type 2 iodothyronine deiodinase (D2) is mediated via an association between mammalian UBC7 and the carboxyl region of D2. Mol. Endocrinol. **17:**2603–2612.
23. **Leonard, J. L., G. Simpson, and D. M. Leonard.** 2005. Characterization of the protein dimerization domain responsible for assembly of functional selenodeiodinases. J. Biol. Chem. **280:**11093–11100.
24. **Ng, L., R. J. Goodyear, C. A. Woods, M. J. Schneider, E. Diamond, G. P.**

Richardson, M. W. Kelley, D. L. Germain, V. A. Galton, and D. Forrest. 2004. Hearing loss and retarded cochlear development in mice lacking type 2 iodothyronine deiodinase. Proc. Natl. Acad. Sci. USA **101:**3474–3479.

25. **Pines, J., and C. Lindon.** 2005. Proteolysis: anytime, any place, anywhere? Nat. Cell Biol. **7:**731–735.
26. **Ravid, T., S. G. Kreft, and M. Hochstrasser.** 2006. Membrane and soluble substrates of the Doa10 ubiquitin ligase are degraded by distinct pathways. EMBO J. **25:**533–543.
27. **Silva, J. E., and P. R. Larsen.** 1983. Adrenergic activation of triiodothyronine production in brown adipose tissue. Nature **305:**712–713.
28. **Steinsapir, J., A. C. Bianco, C. Buettner, J. Harney, and P. R. Larsen.** 2000. Substrate-induced down-regulation of human type 2 deiodinase (hD2) is mediated through proteasomal degradation and requires interaction with the enzyme's active center. Endocrinology **141:**1127–1135.
29. **Steinsapir, J., J. Harney, and P. R. Larsen.** 1998. Type 2 iodothyronine deiodinase in rat pituitary tumor cells is inactivated in proteasomes. J. Clin. Investig. **102:**1895–1899.
30. **Toyoda, N., A. M. Zavacki, A. L. Maia, J. W. Harney, and P. R. Larsen.** 1995. A novel retinoid X receptor-independent thyroid hormone response element is present in the human type 1 deiodinase gene. Mol. Cell. Biol. **15:**5100–5112.
31. **Watanabe, M., S. M. Houten, C. Mataki, M. A. Christoffolete, B. W. Kim, H. Sato, N. Messaddeq, J. W. Harney, O. Ezaki, T. Kodama, K. Schoonjans, A. C. Bianco, and J. Auwerx.** 2006. Bile acids induce energy expenditure by promoting intracellular thyroid hormone activation. Nature **439:**484–489.
32. **Weichsel, A., J. R. Gasdaska, G. Powis, and W. R. Montfort.** 1996. Crystal structures of reduced, oxidized, and mutated human thioredoxins: evidence for a regulatory homodimer. Structure **4:**735–751.
33. **Yoshimura, T., S. Yasuo, M. Watanabe, M. Iigo, T. Yamamura, K. Hirunagi, and S. Ebihara.** 2003. Light-induced hormone conversion of T4 to T3 regulates photoperiodic response of gonads in birds. Nature **426:**178–181.
34. **Zheng, N., B. A. Schulman, L. Song, J. J. Miller, P. D. Jeffrey, P. Wang, C. Chu, D. M. Koepp, S. J. Elledge, M. Pagano, R. C. Conaway, J. W. Conaway, J. W. Harper, and N. P. Pavletich.** 2002. Structure of the Cul1-Rbx1-Skp1-F boxSkp2 SCF ubiquitin ligase complex. Nature **416:**703–709.